A model for kinetically controlled internal phase segregation during aerosol coagulation

H. Struchtrup [1], M. Luskin, M. R. Zachariah*

University of Minnesota, Minneapolis, MN 55455, USA

Abstract

In previous studies of particle growth, we have synthesized binary metal oxide aerosols and have observed the evolution of internal phase segregation during growth of molten nanodroplets. We describe a new formulation of the aerosol general dynamic equation (GDE) that incorporates phase segregation in a binary aerosol. The model assumes that complete phase segregation is the thermodynamically favored state, that no thermodynamic activation energy exists, and that the segregation process is kinetically controlled. We develop a GDE formulation that involves the solution of a distribution function $N_n(V)$, where $N_n(V)$ is the number density of aerosols with volume V and n phase domains (which we might think of as enclosures). The GDE is solved using a two-dimensional sectional model, under the assumption that the phase coalescence of the minority phase is controlled by Brownian coagulation. For the purposes of these initial studies, the rate laws governing the enclosures (minority phase) assume a monodisperse particle size distribution. The dynamical behavior of such a system is presented. © 2001 Elsevier Science Ltd. All rights reserved.

Keywords: Coagulation; General dynamic equation; Metal oxides; Phase segregation

1. Introduction

The evolution of an aerosol population is described by a master equation, the "aerosol general dynamic equation" (GDE). The GDE has been employed to characterize the behavior in time and space of the particle size distribution function, which can include all the driving forces for

---

* Corresponding author. Tel.: +1-612-626-9081; fax: 1-612-625-6069.

E-mail addresses: struchtr@me.uvic.ca (H. Struchtrup), luskin@math.umn.edu (M. Luskin), mrz@me.umn.edu (M.R. Zachariah).

[1] Permanent Address: Department of Mechanical Engineering, University of Victoria, Victoria BC V8W 3P6, Canada.
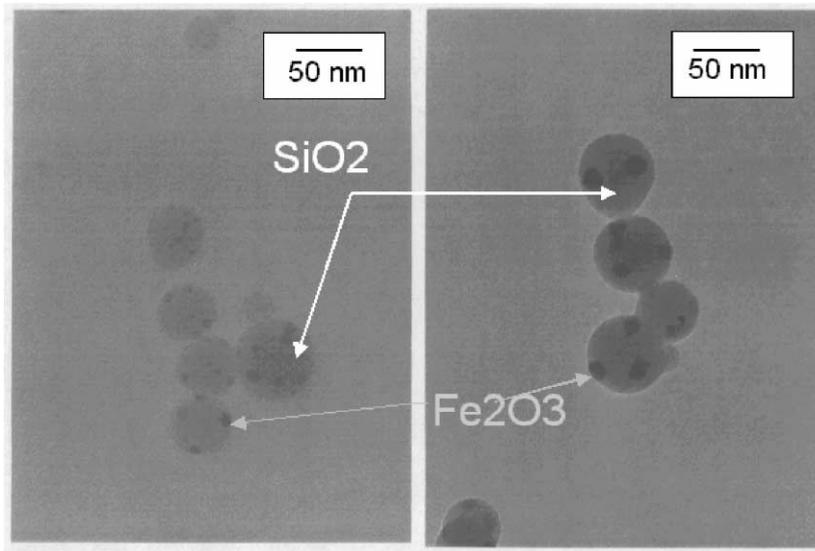
Fig. 1. Aerosol droplet with enclosures. The droplets on the left are "younger".

particle growth (nucleation, surface growth, coagulation/coalescence, transport) (Friedlander, 2000).

However, in these multi-component studies it is assumed that the components comprising the particles are homogeneously distributed within the particle. We have been involved in a number of multi-component aerosol dynamics studies in which the internal structure of the components within the aerosol particle are at the heart of our interest in the materials, their properties and function. For example, we have conducted studies on the formation of binary metal oxide systems with application to removal of heavy metals (Biswas & Zachariah, 1997; Biswas, Yang, & Zachariah, 1998) as well as the formation of materials with novel and interesting properties (Ehrman, Friedlander, & Zachariah, 1998, 1999; Ehrman, Aquino-Class, & Zachariah, 1999).

In this study, we focus on one particular binary system (SiO_2/Fe_2O_3) which we have studied in considerable detail. For this iron oxide/silica system, our initial goal was to develop a method for producing a ferromagnetic cluster within a non-magnetic host, and the iron oxide/silica system was chosen because the phase behavior at very high temperatures, that is when both components are in the liquid state, indicated that the liquids would be immiscible.

Our initial success in producing these materials (Zachariah, Aquino-Class, Shull, & Steel, 1995) indicated that further research into the mechanistic aspects of the growth was warranted. In subsequent studies, we employed both in situ interrogation into the formation process (McMillin, Biswas, & Zachariah, 1996), multi-component aerosol dynamic modeling (Biswas, Wu, Zachariah, & McMillen, 1997), and molecular dynamics computation (Zachariah, Shull, McMillin, & Biswas, 1996). One of the primary conclusions from these works was that at these high temperatures, where the nanodroplets are in a liquid like state, the phase segregation taking place within the nanodroplet was probably driven by a kinetically limited transport within the nanodroplet. Fig. 1 shows TEM images of these nanocomposites at two different growth times.
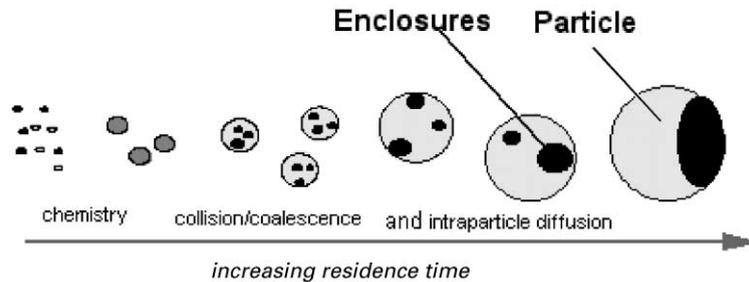
Fig. 2. Schematic representation of the temporal evolution of a two component aerosol.

The images make clear the existence of dark (Fe_2O_3) and light (SiO_2) domains, in which with increasing time we see the growth of the iron oxide phase. One can imagine that the temporal evolution of the aerosol phase follows the general characteristics illustrated in Fig. 2.

Our goal in this paper is to develop a new formulation of the GDE which characterizes both aerosol growth, and the evolution of the internal morphology of multi-component liquid aerosols in which the phases are immiscible.

Formulation of the GDE for the problem presented is a variant in the formulation of other 2-D GDEs that have been used to track both composition and shape. In (Koch, & Friedlander, 1990) a multi-component formulation treats the changes in composition of particles, but assumes each aerosol particle to be homogeneous. Other approaches treat the evolution in shape due to finite coalescence events (Koch, & Friedlander, 1990; Xiong & Pratsinis, 1993). In the present formulation we assume instantaneous coalescence with a multi-component formulation which assume that the particle interior is inhomogeneous.

The model developed in this paper must be considered as the first step towards a more detailed theory which—hopefully—will be able to describe experimental observations. In its present state, the model relies on many assumptions, however, the experiments themselves are of a sufficiently qualitative nature that quantitative comparison is unwarranted. Rather we hope to develop the model and explain the qualitative behavior observed and conclude some generic results associated with processes of this type.

2. The model

Due to surface tension, the iron oxide phase forms sphere-like enclosures inside the aerosol droplets. Obviously, it is not possible to describe the individual enclosures inside individual droplets since the numerical efforts would be tremendous. Therefore, we supplement the usual statistical formulation for the droplets, as given by the GDE, with terms which account for the statistics of the iron oxide enclosures.

The enclosures are considered as particles inside the molten droplet, where coagulation takes place due to the Brownian motion of the enclosures. In this first approach to the problem, we only account for the expected number of enclosures inside the droplets. Thus, we ignore most details of the physics inside the droplet. In particular, we do not account for the size distribution of the enclosures.

Furthermore, to make the initial development of the model more tractable, we assume that the characteristic time for nucleation is considerably shorter than the subsequent growth processes. Implicit is that both components do not have significantly different nucleation rates. These latter points are quite reasonable based on our prior in situ and modeling studies (see references above). Under such conditions, we assume that we have no gas–solid material transfer, so that the only physical/chemical processes occurring are inter- and intra-aerosol transfer processes. Finally, we also assume that the solubility of either component in the other is so small that enclosures cannot loose material by dissolution processes. Under this assumptions we can consider the coagulation of existing particles without further reference to nucleation and condensation phenomena.

We consider aerosol droplets which consists of two immiscible components in a constant volume ratio, c. Our objective is the determination of the distribution of droplet volumes in time *and* the internal state of the droplet, that is, the number and size of enclosures in the droplets.

For this first paper, we restrict ourselves to the simplest case and ask for the number density $N_n(t, V) \, \mathrm{d}V$ of droplets with volumes in $(V, V + \mathrm{d}V)$ and n enclosures at time t. In particular, we ignore the size distribution of enclosures, which therefore in a droplet of volume V with n enclosures have the volume cV/n. For simplicity, we shall write $N_n(t, V)$ as the number density distribution as a function of time.

The number density of particles with volume V and *any* number of enclosures is given by

$$\mathcal{N}(t, V) = \sum_{n=1}^{\infty} N_n(t, V). \tag{1}$$

The theory for this quantity is well developed, and one finds an evolution equation for $\mathcal{N}$, the Smoluchowski equation, which reads (Friedlander, 2000)

$$\frac{\mathrm{d}\mathcal{N}(t, V)}{\mathrm{d}t} = \frac{1}{2} \int_0^V \sigma(U, V - U)\mathcal{N}(t, U)\mathcal{N}(t, V - U) \, \mathrm{d}U$$

$$- \mathcal{N}(t, V) \int_0^{\infty} \sigma(V, U)\mathcal{N}(t, U) \, \mathrm{d}U. \tag{2}$$

Here, $\sigma(V, U)$ is the collision probability for droplets with the volumes V and U. Assuming that no friction forces are exerted on the particles during their flight and that their velocities are distributed according to the Maxwell distribution, one finds σ as (Park, Lee, Otto, & Fissan, 1999)

$$\sigma(V, U) = \left(\frac{3}{4\pi}\right)^{1/6} \left(\frac{6kT}{\varrho}\right)^{1/2} \left(\frac{1}{V} + \frac{1}{U}\right)^{1/2} (V^{1/3} + U^{1/3})^2,$$

where k denotes Boltzmann's constant, T is the temperature and ϱ is the mass density of the droplets. The first term in the right-hand side of Eq. (2) accounts for the gain of particles with volume V due to agglomeration of particles with volumes U and $V - U$, while the second accounts for the loss due to agglomeration of droplets with volume V and droplets with any other volume.

We shall now construct the corresponding equation for $N_n(t, V)$. Under the natural assumption that the collision probability $\sigma(V, U)$ does not depend on the number of enclosures, we have (time dependence suppressed in the notation)

$$\frac{\mathrm{d}N_n(V)}{\mathrm{d}t} = \frac{1}{2} \int_0^V \sigma(U, V - U) \sum_{m=1}^{n-1} N_m(U) N_{n-m}(V - U) \, \mathrm{d}U$$

$$- N_n(V) \int_0^\infty \sigma(V, U) \sum_{m=1}^\infty N_m(U) \, \mathrm{d}U$$

$$+ \sum_{m=n+1}^\infty \gamma_{m \to n}(V) N_m(V) - \sum_{m=1}^{n-1} \gamma_{n \to m}(V) N_n(V). \tag{3}$$

Here, again, the first two terms account for the gain and loss due to the agglomeration of *droplets*, while the last two terms refer to the gain and loss due to the coagulation of *enclosures* inside a droplet of volume V. The quantity $\gamma_{n \to m}(V) \, \mathrm{d}t$ denotes the probability that in a droplet of volume V the number of enclosures will change from n to m during the time $\mathrm{d}t$; this quantity will be considered in the next section.

The coagulation equation (3) has two conservative properties:

1. The coagulation of enclosures does not change the total number $\mathcal{N}(t, V)$ as defined in Eq. (1), so that the summation of Eq. (3) over all n gives the proper equation (2) for $\mathcal{N}(t, V)$. The simple proof relies on the fact that one can invert the sequence of summation as

$$\sum_{n=1}^\infty \sum_{m=1}^{n-1} = \sum_{m=1}^\infty \sum_{n=m+1}^\infty .$$

2. The total volume density

$$v_{\mathrm{tot}}(t) = \sum_n \int V N_n(t, V) \, \mathrm{d}V = \int V \mathcal{N}(t, V) \, \mathrm{d}V \tag{4}$$

is constant in time, that is, $v_{\mathrm{tot}}(t) = v_{\mathrm{tot}}(0) = constant$. This is readily shown by multiplication of (2) with the volume V and subsequent integration.

3. Collision probability for enclosures

3.1. Mean time for agglomeration

By definition, $1/\gamma_{n \to m}(V)$ is the mean time for the change of the number of enclosures from n to m in a droplet of size V. For the calculation of this time, we assume that Brownian motion of the enclosures is the dominant physical process inside the droplet. Other possible growth mechanisms, such as Oswald ripening, are considered to play no important role. Moreover, in

our simple model we do not account for the different volumes of the enclosures which are assumed to be spherical.

The theory of the coagulation of spherical particles of the same size provides a differential equation for their number density $v = n/V$ which reads (Fuchs, 1989)

$$\frac{\mathrm{d}v}{\mathrm{d}t} = -K_0 v^2 \quad \text{with } K_0 = \kappa \frac{kT}{\eta}, \tag{5}$$

where η denotes the viscosity of the surrounding medium (the silica in our case) and κ is a number that for the case of rigid particles moving in a gas (Fuchs, 1989) has the value $\kappa = \frac{4}{3}$. In our case, however, the deformable enclosures move in a liquid. Moreover, Eq. (5) does not consider the finite size of the droplet and requires that the mean distance between enclosures is considerably smaller than the radius of the droplet. We assume that all aberrations from the ideal conditions for the validity of Eq. (5) can be absorbed into the number, κ. Thus, we have to consider κ as a quantity to be determined by experiments. Nevertheless, due to lack of experimental data, we shall set $\kappa = \frac{4}{3}$. As long as κ can be considered as a constant, its actual value is only of minor importance. A change in κ will not change our results qualitatively. A more detailed theory might yield a dependence of κ—and therefore of K_0—on dropletsize V and enclosure number density v, which would change the subsequent argumentation. Future research will give more insight into these matters.

The right-hand side of Eq. (5) denotes the rate of change of the number density. The probability to find two particles at the same place is proportional to the square of the number density, and thus the rate of change must be proportional to v^2. Moreover, the increase of the temperature increases the movement of the particles due to Brownian motion while a higher viscosity acts against any movement. This explains the factor kT/η in the rate of change.

Eq. (5) can be integrated easily and the solution reads after introducing the particle number $v = n/V$

$$n = \frac{n_0}{1 + (K_0/V) n_0 t},$$

where n_0 is the number of enclosures at time $t = 0$. It follows that the inverse mean time for the agglomeration of m enclosures to n enclosures in a droplet of volume V, that is, the desired quantity γ, is given by

$$\frac{1}{t_{m \to n}} = \gamma_{m \to n}(V) = \frac{K_0}{V} \frac{nm}{m - n}. \tag{6}$$

Thus, the probability of agglomeration increases with increasing K_0 (increasing temperature, decreasing viscosity) and decreases with increasing volume V (increasing mean distance between particles). Moreover, large changes in the number of enclosures are less probable. Note that γ is only needed in Eq. (3) for $n \neq m$, so that it is always finite.

It is remarkable that $\gamma_{m \to n}(V)$ depends only on the number of enclosures n, but not on their volume cV/n. Indeed, the concentration c will not appear in the sequel. This is due to the simple model for the coagulation of the enclosures and will change if a more realistic model is used. A very simple way to bring the concentration into play is discussed briefly in Appendix A.

3.2. Coagulation of enclosures alone

In order to get a glance on the behavior of the enclosures, we consider collision-free droplets of volume $V = V_0$. In Eq. (3), we set $N_n(V) = N_n \delta(V - V_0)$ and $\sigma = 0$ (where $\delta(V)$ is the Dirac delta function) and obtain with Eq. (6)

$$\frac{\mathrm{d}N_n}{\mathrm{d}t} = \sum_{m=n+1}^{\infty} \frac{K_0}{V_0} \frac{nm}{m-n} N_m - \sum_{m=1}^{n-1} \frac{K_0}{V_0} \frac{nm}{n-m} N_n. \tag{7}$$

In actual numerical calculations, we have to restrict the maximum number of enclosures to some finite value, $n_{\max}$. For convenience, we introduce the dimensionless time $\hat{t} = t K_0 / V_0$ so that the equation for coagulation of enclosures can be written as

$$\frac{\mathrm{d}N_n}{\mathrm{d}\hat{t}} = \sum_{m=1}^{n_{\max}} \mathscr{A}_{nm} N_m, \quad n = 1, 2, \ldots, n_{\max}. \tag{8}$$

The matrix $\mathscr{A}_{nm}$ is given by

$$\mathscr{A}_{nm} = \begin{cases} \frac{nm}{m-n}, & m > n, \\ -\sum_{k=1}^{n-1} \frac{kn}{n-k}, & m = n, \\ 0, & m < n. \end{cases} \tag{9}$$

It should be noted that the variable $N_{n_{\max}}$ will always decrease with a characteristic time given by $1/\omega_{n_{\max}}$ where $\omega_n = \sum_{k=1}^{n-1} kn/(n-k)$, while the number N_1 will always grow since $\omega_1 = 0$. Due to the conservation of the number density, we have for $n_{\max} \geqslant m$ that

$$\sum_{n=1}^{n_{\max}} \mathscr{A}_{nm} = \sum_{n=1}^{m} \mathscr{A}_{nm} = 0. \tag{10}$$

In principle, the set (8) of coupled ODEs can be solved by transformation to the principal axes. In practice, however, the large number of equations makes the transformation impossible, and we shall rely on numerical solutions.

The eigenvalues of $\mathscr{A}$ determine the characteristic time scales of the equations, and, due to the simple structure of the matrix, it is easy to state that these are given by the quantities ω_n, that is, the rate of decrease of the number densities N_n. Obviously, the characteristic time scales cover a wide range of values: the number of droplets with a large number of enclosures will decrease much faster than the number of droplets with few enclosures.

This behavior allows for an adaptation of the time step during the numerical calculation. The initial time step $\delta\hat{t}$ is defined by the fastest scale

$$\delta\hat{t} = a/\omega_{n_{\max}},$$

where $a < 1$ is an appropriate constant; for our calculations we chose $a = 0.02$. The number $N_{n_{\max}}$ will decrease and after several time steps its value will fall below a threshold Δ, that is

$$N_{n_{\max}} < \Delta \bar{N} \quad \text{with} \quad \bar{N} = \frac{N_{\text{tot}}}{n_{\max}}, \quad N_{\text{tot}} = \sum_{n=1}^{n_{\max}} N_n \qquad (11)$$

here we chose $\Delta = 0.05$. If this condition is met, the number density $N_{n_{\max}}$ will not contribute significantly to the future process and will be ignored, that is, the corresponding equation will be canceled. Thus, there is not much change during the corresponding time scale $1/\omega_{n_{\max}}$, while the relevant time scale is now given by $\delta\hat{t}_1 = a/\omega_{n_{\max}-1}$. The calculation proceeds until $N_{n_{\max}-1}$ falls below the threshold, $N_{n_{\max}-1} < \Delta \bar{N}$. Then, again, the equation for $N_{n_{\max}-1}$ is ignored, and the new time scale is given by $\delta\hat{t}_2 = a/\omega_{n_{\max}-2}$.

This procedure is carried on until $N_2 < \Delta \bar{N}$, which corresponds to the stationary state, where all droplets have only one enclosure, $N_1 = N_{\text{tot}}$. With this scheme, the number density of droplets with n enclosures ($n \geqslant 2$) is not equal to zero in the stationary state, but given by $N_n^{\text{stat}} \simeq \Delta \bar{N}$, $n \geqslant 2$ and $N_1^{\text{stat}} = (1 - \Delta)N_{\text{tot}}$. Thus, Δ is directly related to the error that is introduced by the method.

Fig. 3 shows the temporal development of N_n/N_{tot} for the normalized initial condition $N_{n_{\max}}(\tau = 0) = 1$, $N_n(\tau = 0) = 0$ ($n < n_{\max}$) with $n_{\max} = 2000$. The pictures were taken in intervals of 1200 time steps. Note that the actual time between the pictures almost quadruples, due to the increase of the time step. With the data given, we find for the stationary values of the number densities $N_n^{\text{stat}} \simeq 2.5 \times 10^{-5}$—this value cannot be resolved on the chosen scale. A further reduction of the threshold Δ does not change the results significantly but will increase the computing time considerably.

3.3. An estimate for the maximum number of enclosures $n_{\max}$

The question of what number $n_{\max}$ we have to choose is closely related to the time scales of the process. For the following, we shall assume that the relevant time scale is given by the mean free time of the droplets. The mean free time is defined as the average time a droplet travels before collision. With the mean volume $\bar{V} = (4\pi/3)\bar{r}^3$ of the droplets and a total number density N_{tot}, the mean free time of the droplets can be approximated as

$$\tau_{\text{D}} = \frac{1}{\sigma(\bar{V}, \bar{V})N_{\text{tot}}}.$$

As an example, we consider an aerosol with $\bar{r} = 50 \times 10^{-9}$ m and $N_{\text{tot}} = 10^{18}$ m^{-3}. We obtain for silica ($\varrho \simeq 2000$ kg m^{-3}) at $T = 2300$ K that

$$\tau_{\text{D}} \simeq 8.10 \times 10^{-5} \text{ s}.$$

We assume that processes on faster scales cannot be measured or are not of interest, respectively. Thus, only those characteristic times τ_n are important for the simulation of the enclosures which are of the same order of magnitude or larger, that is

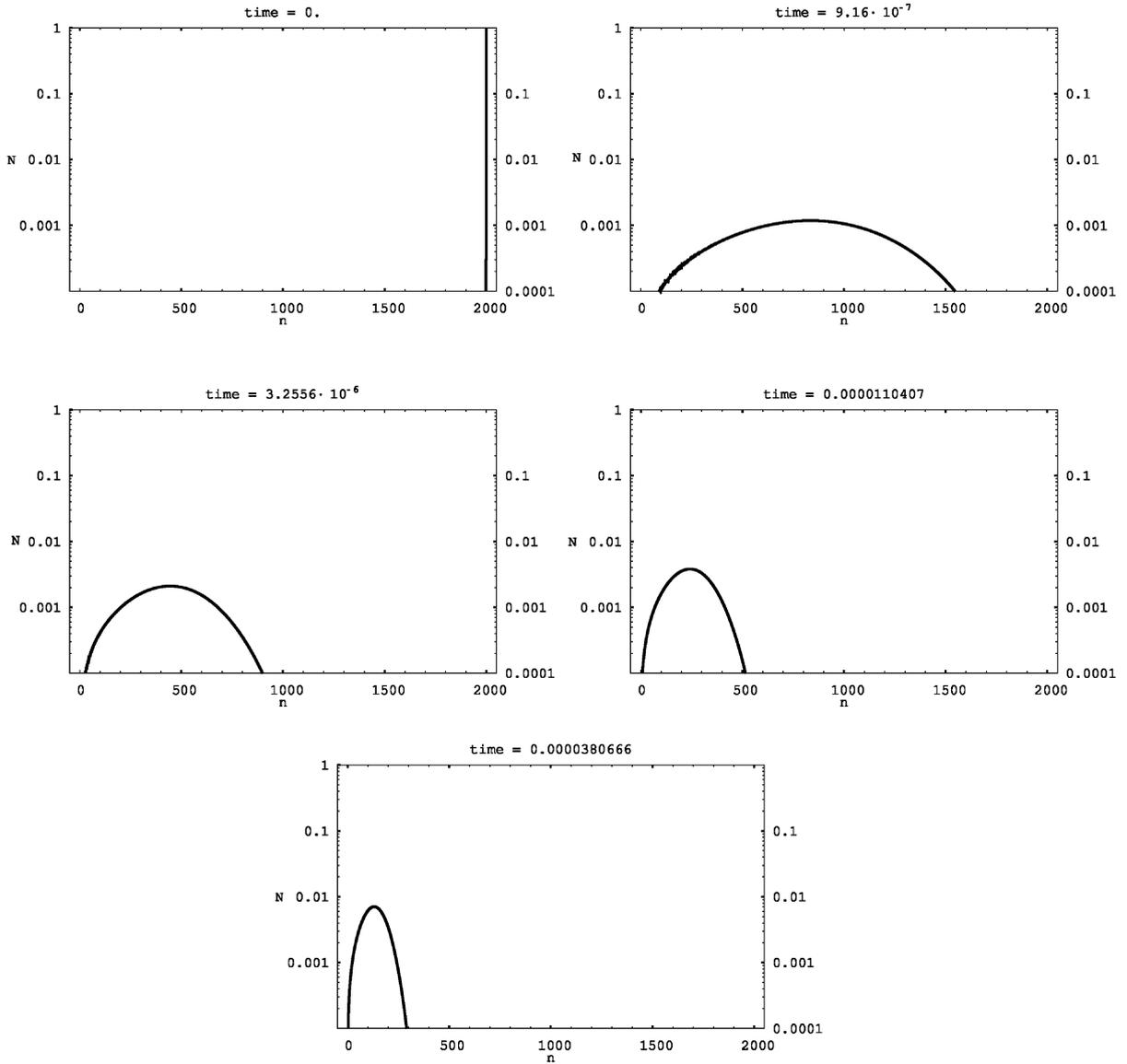$$\tau_n = \frac{V}{K_0} \frac{1}{\omega_n} \geqslant \tau_{\text{D}}, \quad n = 2, 3, \dots .$$

Fig. 3. Distribution of droplets with n enclosures for various times. $n_{\max} = 2000$, droplet number normalized such that initial conditions $N_{n_{\max}}(0) = 1$, $N_n(0) = 0$.

The fastest scale is given by the characteristic time $\tau_{n_{\max}}$ and thus $n_{\max}$ follows as the solution of

$$\tau_{n_{\max}} = \tau_{\mathrm{D}}.$$

Fig. 4 shows the characteristic times τ_n computed for silica at $T = 2300$ K ($\eta \simeq 53776.3$ kg ms^{-1}) as well as the mean free time τ_{D}. The intersection of the curves gives the number $n_{\max} \simeq 1110$, and we conclude that we can ignore droplets with more than 1110 enclosures on the time scale
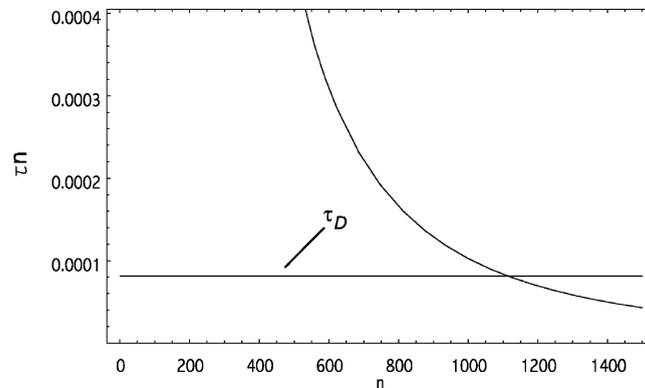
Fig. 4. Characteristic times τ_n and τ_D for silica droplet of radius 50 nm at $T = 2300$ K (in seconds). The intersection of the curves defines $n_{\max} \simeq 1110$.

in question. Of course, this number changes with temperature and droplet radius, and must be considered as a rough estimate.

The number of variables is by far too large for numerical computations and must be reduced.

4. Reduction of variables

4.1. Number of enclosures

In the present problem of coagulation, we have to consider the variables $N_n(V)$. A numerical solution requires discrete values V_A for the volumes, and the number of variables N_n^A might be extremely large, even if the maximum number of enclosures were small. Therefore, it is essential to reduce the number of variables.

To this objective it is reasonable to subsume droplets with adjacent numbers of enclosures into classes. These classes must not be of the same size. Indeed, it makes a big difference, whether a droplet contains 10 or 20 enclosures, while nobody would differentiate between two droplets with 10,000 and 10,010 enclosures. We shall use classes which contain an increasing number of enclosures.

We indicate the classes by Greek indices, $\alpha = 1, 2, \ldots, \alpha_{\max}$, and denote the number of members in class α by μ_α. Moreover, we define the boundaries of the classes by

$$M_\alpha = \sum_{\beta=1}^{\alpha} \mu_\beta \quad \text{for } \alpha = 1, 2, \ldots, \alpha_{\max}, \quad \text{with } M_0 = 0.$$

There are no limitations for the choice of the class widths, μ_α. It turns out, however, that the doubling of the number of members of successive classes allows for simplifications of the subsequent calculations, and thus we set

$$\mu_\alpha = 2^{\alpha-2} \quad \text{for } \alpha = 2, \ldots, \alpha_{\max} \text{ so that } M_\alpha = 2^{\alpha-1} \text{ for } \alpha = 1, \ldots, \alpha_{\max}. \tag{12}$$

Obviously, we must have $M_{\alpha_{\max}} = n_{\max}$ and with the maximal number of enclosures given by $n_{\max} \simeq 1100$, we have $\alpha_{\max} = 11$.

With these definitions, we have for the number densities of droplets in class α

$$v_\alpha(V) = \sum_{n=M_{\alpha-1}+1}^{M_\alpha} N_n(V) \quad \text{for } \alpha = 1, 2, \ldots, \alpha_{\max}.$$

Correspondingly, if the number density lies in class α it will be replaced by the mean number density, that is

$$N_n(V) = \frac{v_\alpha(V)}{\mu_a}, \quad n \in \{M_{\alpha-1} + 1, \ldots, M_\alpha\}. \tag{13}$$

The evolution equation for $v_\alpha(V)$ follows from summation of Eq. (3), and after some rearrangements we obtain

$$\frac{\mathrm{d}v_\alpha(V)}{\mathrm{d}t} = I_{\alpha-1,\alpha-1}(V) + \sum_{\beta=1}^{\alpha-1} (1 - \mathscr{B}_{\alpha\beta})[I_{\alpha\beta}(V) + I_{\beta\alpha}(V)]$$

$$+ \sum_{\beta=1}^{\alpha-2} \mathscr{B}_{\alpha-1,\beta}[I_{\alpha-1,\beta}(V) + I_{\beta,\alpha-1}(V)]$$

$$- \sum_{\beta=1}^{\alpha_{\max}} v_\alpha(V) \int_0^\infty \sigma(V, U) v_\beta(U) \, \mathrm{d}U + K_0 \sum_{\beta=1}^{\alpha_{\max}} \mathscr{A}_{\alpha\beta} \frac{v_\beta(V)}{V}, \tag{14}$$

where we have abbreviated

$$I_{\alpha\beta}(V) = \frac{1}{2} \int_0^V \sigma(U, V - U) v_\alpha(U) v_\beta(V - U) \, \mathrm{d}U \quad \text{with } I_{00}(V) = 0. \tag{15}$$

The matrix $\mathscr{A}_{\alpha\beta}$ is given by sums of elements of the matrix $\mathscr{A}_{nm}$,

$$\mathscr{A}_{\alpha\beta} = \begin{cases} \dfrac{1}{\mu_\beta} \displaystyle\sum_{n=1+M_{\alpha-1}}^{M_\alpha} \sum_{m=1+M_{\beta-1}}^{M_\beta} \dfrac{nm}{m-n}, & \beta > \alpha, \\[2em] -\dfrac{1}{\mu_\alpha} \displaystyle\sum_{n=1+M_{\alpha-1}}^{M_\alpha} \sum_{m=1}^{M_{\alpha-1}} \dfrac{nm}{n-m}, & \beta = \alpha, \\[2em] 0, & \beta < \alpha, \end{cases} \tag{16}$$

where $\omega_\alpha = 1/\mu_\alpha \sum_{n=1+M_{\alpha-1}}^{M_\alpha} \sum_{m=1}^{M_{\alpha-1}} nm/(n-m)$ is the decay time for the class α. Due to the large numbers involved, the elements of $\mathscr{A}_{\alpha\beta}$ for large values, that is, $\alpha, \beta \gtrsim 10$, should be computed by numerical integration rather than summation. The conservation of droplet number for

non-colliding droplets follows from

$$\sum_{\alpha=1}^{\alpha_{\max}} \mathscr{A}_{\alpha\beta} = \sum_{\alpha=1}^{\beta} \mathscr{A}_{\alpha\beta} = 0 \qquad\qquad (17)$$

for $\alpha_{\max} \geqslant \beta$, and, of course, this must be guaranteed also by numerical approximations to $\mathscr{A}_{\alpha\beta}$. The coefficients $\mathscr{B}_{\alpha\beta}$ are given by

$$\mathscr{B}_{\alpha\beta} = \begin{cases} \dfrac{1}{\mu_\alpha}, & \beta = 1, \\[2mm] \dfrac{3\mu_\beta + 1}{2\mu_\alpha}, & \beta \geqslant 2. \end{cases} \qquad\qquad (18)$$

The relevant calculations, in particular the determination of $\mathscr{A}_{\alpha\beta}$ and $\mathscr{B}_{\alpha\beta}$, are outlined in Appendices B and C.

   It is instructive to interpret the various contributions to the right-hand side of Eq. (14). The first two lines refer to the gain of droplets of volume V in class α. The terms $I_{\alpha\beta}(V)$ refer to collisions of two droplets with number of enclosures in classes α and β that produce a droplet of type (V, α). Note that due to the specific choice of the class width (12) a droplet in α will result only if one of the original droplets is in class α or $(\alpha - 1)$, respectively.

   The next terms refer to the loss of droplets (V, α) due to collisions with any other type of droplets, and to the gain and loss due to agglomeration of enclosures—the off-diagonal elements of $\mathscr{A}_{\alpha\beta}$ refer to the gain and the diagonal terms to the loss.

   Of course, the total number density of droplets with volume V is given by

$$\mathscr{N}(V) = \sum_{\alpha=1}^{\alpha_{\max}} v_a(V).$$

The summation of Eq. (14) over all classes should give the coagulation equation for droplets (2). It is easy to show that this is indeed the case as long as $\alpha_{\max} \to \infty$ or as $v_\alpha(V) \simeq 0$ for $\alpha \geqslant \alpha_{\max}$, respectively. The last condition gives us a useful criterion for the choice of $\alpha_{\max}$: if during the numerical calculation $v_{a_{\max}}$ becomes significantly different from zero, the number $\alpha_{\max}$ is too small for the process under consideration, and must be increased.

4.2. Volume of droplets

   In the last step for the reduction of variables, we subsume the continuous volumes of the droplets into sections, see Landgrebe and Pratsinis (1990) for a thorough survey for the case without enclosures. We indicate the sections by capital indices, $A = 1, 2, \ldots, A_{\max}$, and denote the volumes of the sections by Δ_A. Moreover, we define the boundaries of the sections by

$$V_A = \sum_{B=1}^{A} \Delta_B \quad \text{for } A = 1, 2, \ldots, A_{\max} \quad \text{with } V_0 = 0.$$

Again, the doubling of the volumes of successive sections allows for simplifications of the subsequent calculations (Hunslow, Ryall, & Marshall, 1988), and thus we set

$$\Delta_A = 2^{A-2}\bar{V} \quad \text{for } A = 2, \ldots, A_{\max} \text{ so that } V_A = 2^{A-1}\bar{V} \text{ for } A = 1, \ldots, A_{\max}. \qquad (19)$$

Here, $\bar{V}$ defines the smallest droplet volume of interest and must be chosen according to the process under consideration.

With these definitions, we have for the number densities of droplets with number of enclosures in class α and volume in section A

$$v_\alpha^A = \int_{V_{A-1}}^{V_A} v_\alpha(V)\,dV, \quad A = 1, 2, \ldots, A_{\max}. \tag{20}$$

Correspondingly, if the number density lies in class α and section A, it will be replaced by the mean number density

$$v_\alpha(V) = \frac{v_\alpha^A}{\Delta_A}, \quad V \in (V_{A-1}, V_A). \tag{21}$$

The evolution equation for the number densities v_α^A follows from integration of Eq. (14) over the interval (V_{A-1}, V_A) and reads after some rearrangements

$$\frac{dv_\alpha^A}{dt} = I_{\alpha-1,\alpha-1}^A + \sum_{\beta=1}^{\alpha-1}(1 - \mathcal{B}_{\alpha\beta})[I_{\alpha\beta}^A + I_{\beta\alpha}^A] + \sum_{\beta=1}^{\alpha-2}\mathcal{B}_{\alpha-1,\beta}[I_{\alpha-1,\beta}^A + I_{\beta,\alpha-1}^A]$$

$$- \sum_{\beta=1}^{\alpha_{\max}}\sum_{B=1}^{A_{\max}}\sigma_{AB}v_\alpha^A v_\beta^B + \frac{K_0 \ln 2}{\Delta_A}\sum_{\beta=\alpha}^{\alpha_{\max}}\mathcal{A}_{\alpha\beta}\,v_\beta^A. \tag{22}$$

Some details of the calculation are given in Appendix D. In particular, $I_{\alpha\beta}^A$ is an abbreviation for a non-linear function of the variables v_α^A given by

$$I_{00}^A = 0,$$

$$I_{\alpha\beta}^1 = \frac{1}{2}(\sigma_{11} - \hat{\sigma}_{11})v_\alpha^1 v_\beta^1,$$

$$I_{\alpha\beta}^2 = \frac{1}{2}\hat{\sigma}_{11}v_\alpha^1 v_\beta^1 + \frac{1}{2}(\sigma_{21} - \hat{\sigma}_{21})[v_\alpha^1 v_\beta^2 + v_\alpha^2 v_\beta^1],$$

$$I_{\alpha\beta}^A = \frac{1}{2}\left[\sigma_{A-1,A-1}v_\alpha^{A-1}v_\beta^{A-1} + \sum_{B=1}^{A-2}\hat{\sigma}_{A-1,B}[v_\alpha^{A-1}v_\beta^B + v_\alpha^B v_\beta^{A-1}]\right.$$

$$\left. + \sum_{B=1}^{A-1}(\sigma_{AB} - \hat{\sigma}_{AB})[v_\alpha^A v_\beta^B + v_\alpha^B v_\beta^A]\right] \quad \text{for } A \geqslant 3, \tag{23}$$

where σ_{AB} and $\hat{\sigma}_{AB}$ are mean collision frequencies for the droplets and are computed by

$$\sigma_{AB} = \int_{V_{B-1}}^{V_B}\int_{V_{A-1}}^{V_A}\frac{\sigma(U,W)}{\Delta_A \Delta_B}\,dW\,dU, \quad \hat{\sigma}_{AB} = \int_{V_{B-1}}^{V_B}\int_{V_A-U}^{V_A}\frac{\sigma(U,W)}{\Delta_A \Delta_B}\,dW\,dU. \tag{24}$$

The interpretation of the various terms is as follows: terms in $I_{\alpha\beta}^A$ with σ_{AB}, $\hat{\sigma}_{AB}$ and $\sigma_{A-1,B}$, $\hat{\sigma}_{A-1,B}$ refer to the gain of droplets in section A due to collision of droplets in section A and B or the collision of droplets in $(A-1)$ and B, respectively. Again, the terms in the last line of

Eq. (22) refer to the loss due to collisions of droplets of type (α, A) with any other type (β, B) and to the coagulation of enclosures, described by the matrix $\mathscr{A}_{\alpha\beta}$.

The original equation (3) conserves the total volume density, $v_{\text{tot}}(t)$, as defined in Eq. (4). In terms of the discrete variables v_α^A, where there are different volumes in one section, the total volume density can be computed from

$$v_{\text{tot}}(t) = \sum_{\alpha, A} \bar{V}_A v_\alpha^A.$$

Here, $\bar{V}_A$ is a suitable mean droplet volume associated with Section A. We have not tried to find an analytical expression for $\bar{V}_A$ but found empirically from our numerical data that v_{tot} is almost constant if we use

$$\bar{V}_A = \frac{\left(\int_{V_{A-1}}^{V_A} V^a \, \mathrm{d}V\right)^{1/a}}{\int_{V_{A-1}}^{V_A} \mathrm{d}V} \quad \text{with } a \simeq 1.16. \tag{25}$$

With this choice the total volume is well conserved with an error of less than 1%.

4.3. Dimensionless quantities, time scales

In this section, we introduce dimensionless quantities in order to identify the relevant parameters and timescales of our problem. It is natural to measure the volume in multiples of the volume $\bar{V}$, which is the smallest possible droplet volume. Its value is determined by the initial conditions.

With u, w defined as $U = u\bar{V}$, $W = w\bar{V}$, we can write the collision probability as

$$\sigma(U, W) = \sigma_0 \sigma(u, w),$$

where

$$\sigma_0 = \left(\frac{3}{4\pi}\right)^{1/6} \left(\frac{6kT}{\varrho\bar{V}}\right)^{1/2} \bar{V}^{2/3} \quad \text{and} \quad \sigma(u, w) = \left(\frac{1}{u} + \frac{1}{w}\right)^{1/2} (v^{1/3} + w^{1/3})^2.$$

The dimensionless time is best defined as

$$\tilde{t} = \frac{\sigma_0}{\bar{V}} t$$

and the parameter

$$\tilde{K}_0 = \frac{K_0}{\sigma_0}$$

measures the relative frequency of the coagulation of enclosures. Moreover, we introduce the dimensionless section widths by

$$\delta_A = \Delta_A / \bar{V} \quad \text{and} \quad v_A = V_A / \bar{V} = \sum_{B=1}^{A} \delta_B$$

and replace v_α^A by the dimensionless expression

$$\tilde{v}_\alpha^A = v_\alpha^A \bar{V}. \tag{26}$$

For simplicity of the notation, we omit the tildes from now on, so that the equation in dimensionless units reads

$$\frac{dv_\alpha^A}{dt} = I_{\alpha-1,\alpha-1}^A + \sum_{\beta=1}^{\alpha-1}(1-\mathscr{B}_{\alpha\beta})[I_{\alpha\beta}^A + I_{\beta\alpha}^A] + \sum_{\beta=1}^{\alpha-2}\mathscr{B}_{\alpha-1,\beta}[I_{\alpha-1,\beta}^A + I_{\beta,\alpha-1}^A]$$

$$-\sum_{\beta=1}^{\alpha_{max}}\sum_{B=1}^{A_{max}}\sigma_{AB}v_\alpha^A v_\beta^B + K_0\frac{\ln 2}{\delta_A}\sum_{\beta=\alpha}^{\alpha_{max}}\mathscr{A}_{\alpha\beta}\,v_\beta^A. \tag{27}$$

The dimensionless counterpart of $I_{\alpha\beta}^A$ has exactly the same form as $I_{\alpha\beta}^A$ (23), where now $\sigma_{AB}, \hat{\sigma}_{AB}$ stands for the dimensionless quantities.

$$\sigma_{AB} = \int_{v_{A-1}}^{v_A}\int_{v_{B-1}}^{v_B}\frac{\sigma(u,w)}{\delta_A\delta_B}\,dw\,du, \quad \hat{\sigma}_{AB} = \int_{v_{A-1}}^{v_A}\int_{v_{B-1}-w}^{v_B}\frac{\sigma(u,w)}{\delta_A\delta_B}\,dw\,du.$$

The matrices $\mathscr{A}_{\alpha\beta}$, $\mathscr{B}_{\alpha\beta}$ are numbers, and remain unchanged.

5. Results

We consider a case where initially all droplets have the same volume $\bar{V} = \frac{4}{3}\pi\bar{r}^3$ with a radius $\bar{r} = 5 \times 10^{-9}$ m; the initial number density of droplets is $\mathscr{N}_0(\bar{V}) = 10^{18}$ m^{-3}. For the calculation of K_0, we need the viscosity of silica. Extrapolating data from Kingery et al. (1976, p. 764), we find

$$\eta = 10^{-8.6625(1-3556.03K/T)}\text{ kg ms}^{-1}$$

With this formula, we have for the dimensionless values of K_0 at $T = 2300$ and 2600 K

$$K_0(2300\text{ K}) = 1.14 \times 10^{-9}, \quad K_0(2600\text{ K}) = 4.25 \times 10^{-8}.$$

The initial number of enclosures in the droplets is assumed to be the maximum number we can observe on the time scale defined by the collisions. By the same arguments as in Section 3.3, we obtain for $T = 2300$ K an initial number of $n_{max} \simeq 30$, corresponding to the class $\alpha_{max} = 6$ and for $T = 2600$ K we find $\alpha_{max} = 3$. The corresponding initial condition is given by

$$v_\alpha^A(t=0) = u_0\delta_{A,1}\delta_{\alpha,\alpha_{max}}, \quad u_0 = \bar{V}\mathscr{N}_0(\bar{V}) \simeq 5 \times 10^{-7}.$$

We compute the coagulation process for $T = 2300$ K, accounting for 12 classes and 15 sections, and for $T = 2600$ K accounting for 9 classes and 15 sections, respectively.

The contour plots in Fig. 5 show, for $T = 2300$ K, the temporal development of the aerosol through v_α^A (A: x-axis, α: y-axis). Recall that A is a measure of the drop size and α is a measure of the number of enclosures. We observe the development of a structure which moves in the (A, α)-plane almost without changing its shape. The development of a self-preserving structure is well known for the coagulation process of droplets alone (Friedlander, 2000). Here, we observe a similar behavior for droplets with enclosures.
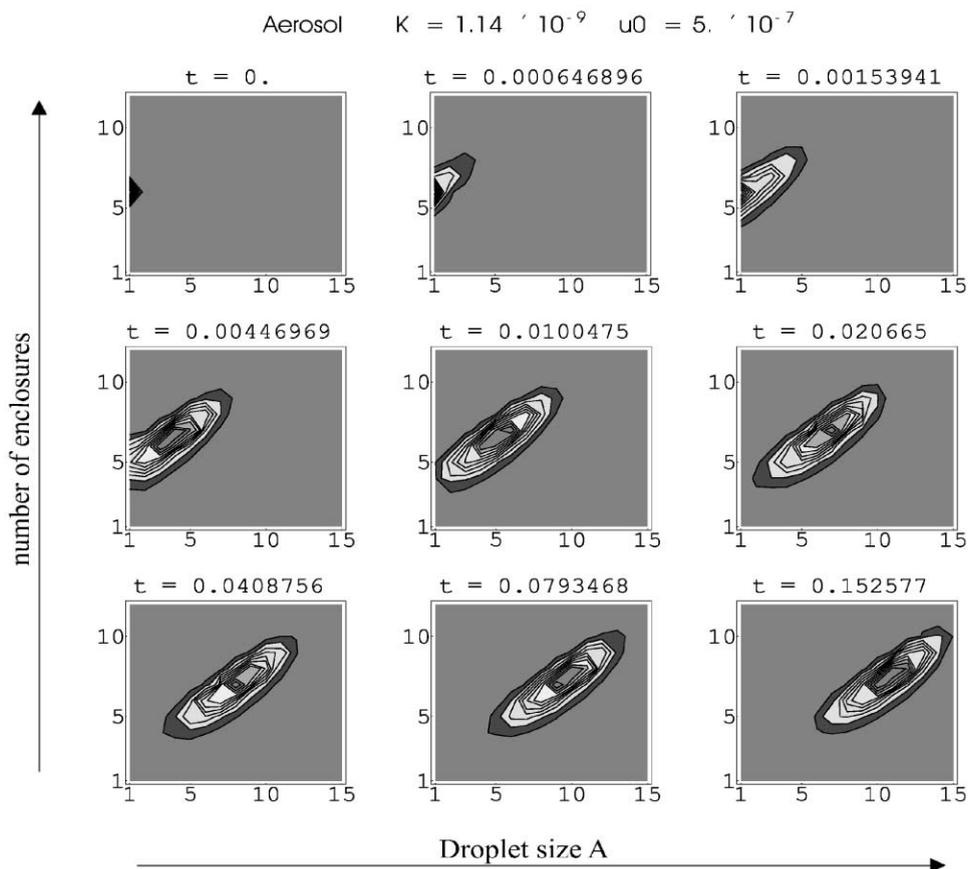
Fig. 5. Temporal evolution of v_α^A for $K = 1.14 \times 10^{-9}$, $u_0 = 5 \times 10^{-7}$ ($T = 2300$ K). Vertical axis: α, horizontal axis: A. The gray levels refer only to the relative values inside one plot. t is the actual time in seconds.

The diagonal shape of the structure becomes clear if one thinks of the relevant growth mechanisms: Droplets with a large volume and a large number of enclosures are those that were newly produced by collisions of smaller droplets with less enclosures. Small droplets vanish due to collisions. And finally, the number of droplets with a large number of enclosures decreases due to enclosure coagulation. Small droplets are those that have encountered fewer collisions, and therefore, their number of enclosures—never increased by collisions, but rather decreased by coagulation—is at the bottom left-hand region of the diagonal structure.

Fig. 6 shows the coagulation process with the same parameters, but for a case where initially all droplets have only one enclosure. At early times, the contour plots differ from those in Fig. 5, but with increasing time, we find the same self-preserving structure as before—the result becomes independent of the initial data.

If one chooses the initial number of enclosures to be larger than n_{max}, one observes first a decrease of the number of enclosures, with no coagulation of droplets, corresponding to the results in Section 3.2. This reflects the difference in the characteristic time scales for the two coagulation processes. When the number of enclosures has decreased to n_{max} as computed in
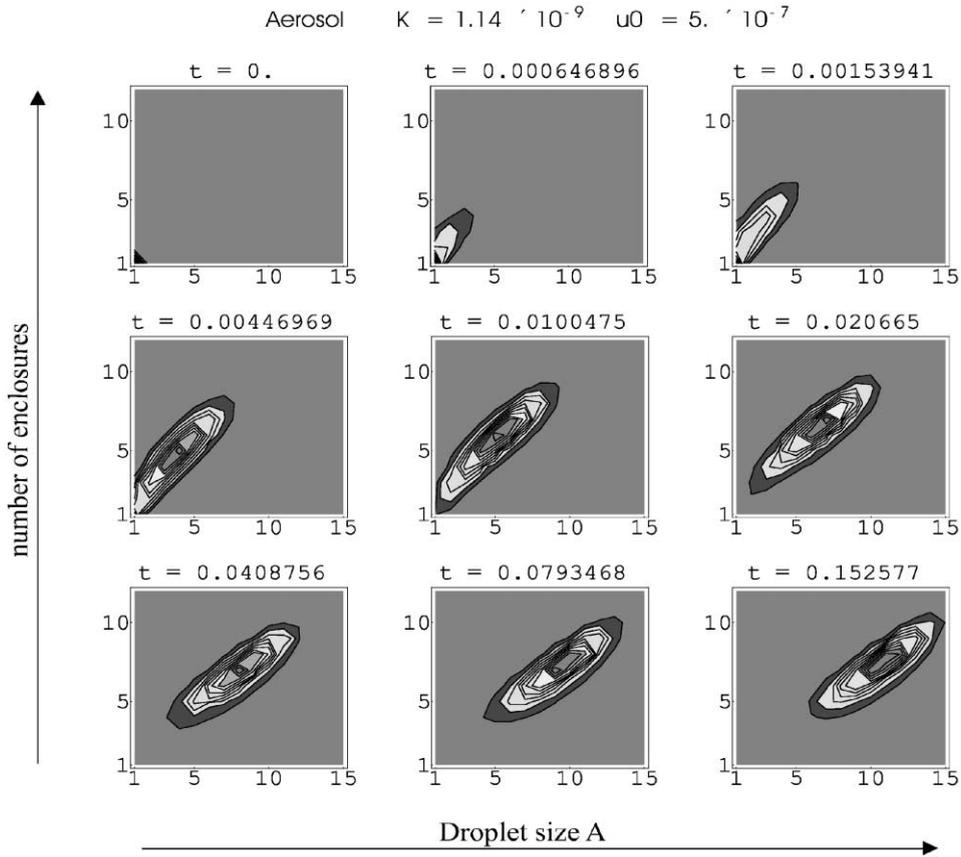
Fig. 6. Temporal evolution of v_α^A for $K = 1.14 \times 10^{-9}$, $u_0 = 5 \times 10^{-7}$ ($T = 2300$ K). Initially all droplets contain 1 enclosure. Vertical axis: α, horizontal axis: A. The gray levels refer only to the relative values inside one plot. t is the actual time in seconds.

Section 3.3, the characteristic times become comparable, the coagulation of droplets sets in, and the results are close to those in Fig. 5.

In Fig. 7 we show the result for $T = 2600$ K. Due to the higher temperature, the enclosures move more easily and thus coagulate more frequently. Therefore, the self-preserving structure is located at lower numbers of enclosures.

In all cases, the structure travels almost horizontally, with a slight ascent towards the right upper corner. Thus, in later times, the number of enclosures per droplet is increasing. In order to make this behavior more evident, Fig. 8 shows the number density of enclosures

$$n_d = \sum_n \int n N_n(V)\,dV \simeq \sum_{\alpha, A} \bar{n}_\alpha v_\alpha^A$$

the mean volume of enclosures

$$\bar{v} = \frac{\sum_n \int cV/n N_n(V)\,dV}{\sum_n \int N_n(V)\,dV} \simeq \frac{\sum_{\alpha, A}(c\bar{V}_A/\bar{n}_\alpha)v_\alpha^A}{\sum_{\alpha, A} v_\alpha^A}$$

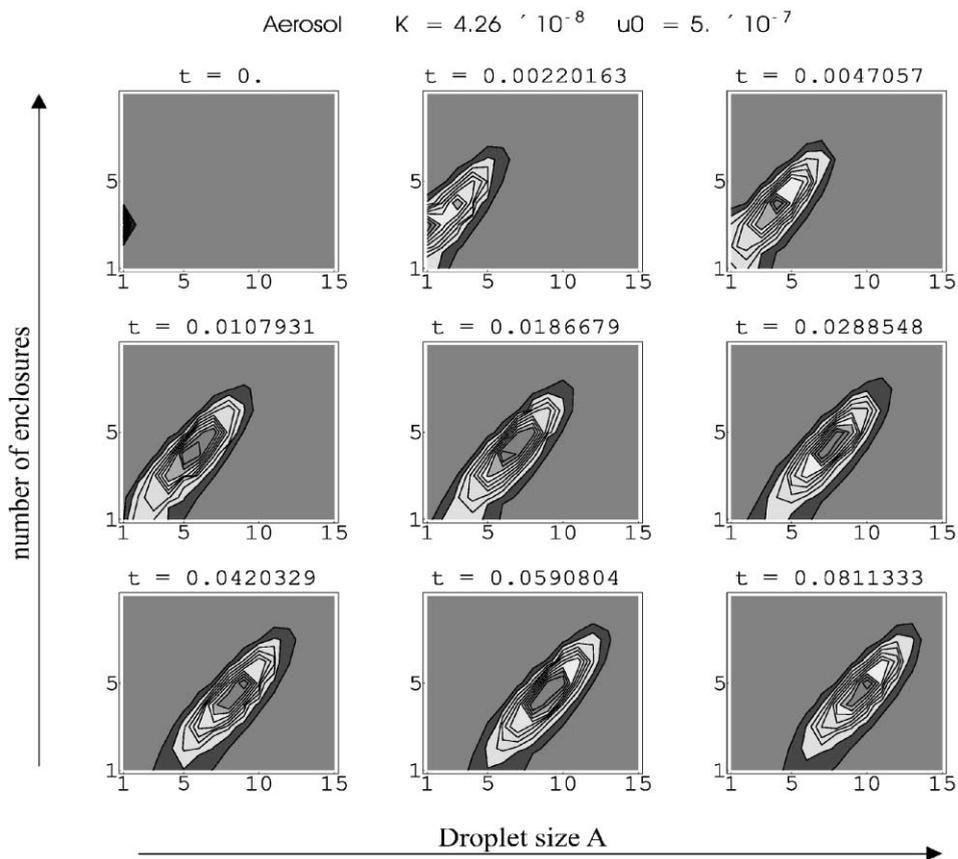Fig. 7. Temporal evolution of v_α^A for $K = 4.25 \times 10^{-8}$, $u_0 = 5 \times 10^{-7}$ ($T = 2600$ K). Vertical axis: α, horizontal axis: A. The gray levels refer only to the relative values inside one plot. t is the actual time in seconds.

and the mean number of enclosures per droplet

$$\bar{n} = \frac{\sum_n \int n N_n(V)\,\mathrm{d}V}{\sum_n \int N_n(V)\,\mathrm{d}V} \simeq \frac{\sum_{\alpha,A} \bar{n}_\alpha v_\alpha^A}{\sum_{\alpha,A} v_\alpha^A}$$

all in dimensionless quantities. $\bar{V}_A$ is the mean volume of droplets in section A, see Eq. (25), and $\bar{n}_\alpha = (2^{\alpha-1} + 2^{\alpha-2})/2$ is the mean number of enclosures in class α. The mean volume was calculated for concentration $c = 0.1$.

The total number density of enclosures decreases due to coagulation (Fig. 8, top), and accordingly the mean volume of the enclosures grows (Fig. 8, middle).

According to our results, the mean number of enclosures per droplet increases in time (Fig. 8, bottom). This is in contradiction to the experimental findings which show a decrease in the number of enclosures at later times, see Figs. 1 and 2. Mathematically, the ascent is related to the term K_0/V in the collision probability for enclosures, $\gamma_{m \to n}$ (6), which means that in larger droplets the enclosures coagulate less frequently. We may conclude that our model for
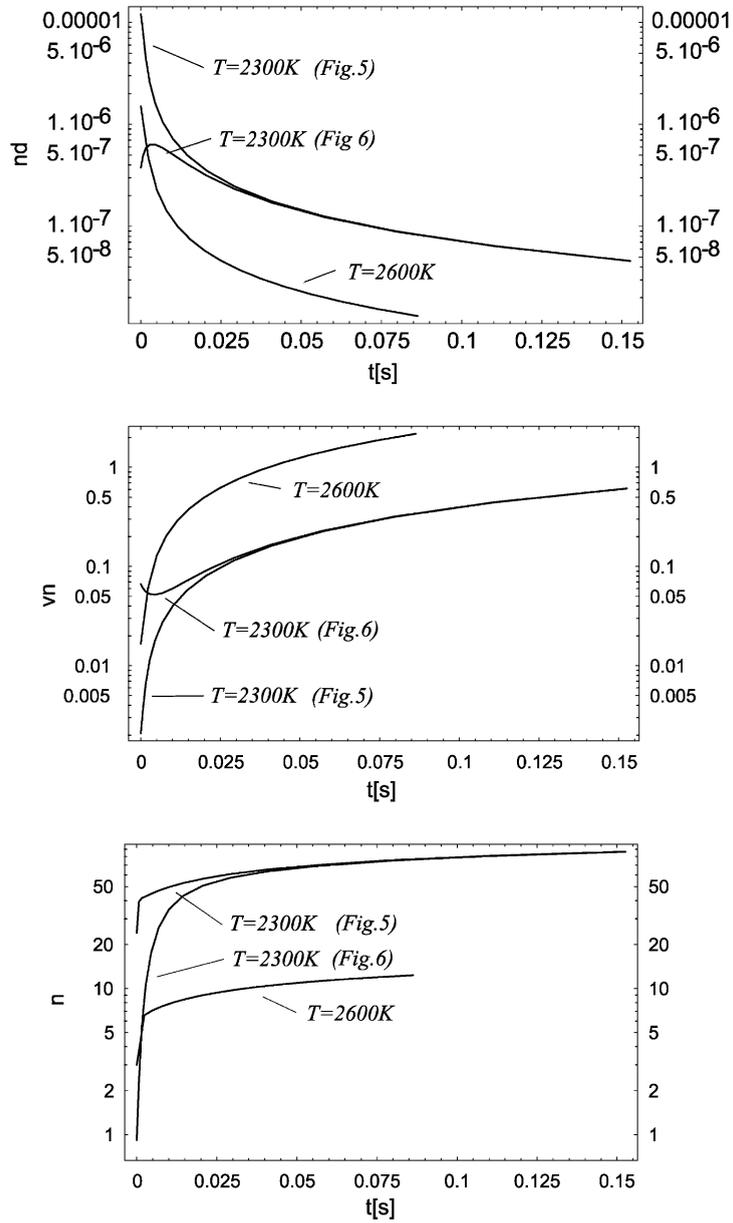
Fig. 8. Enclosure number density (top, dimensionless), enclosure volume (middle, in fractions of the initial droplet size) and mean number of enclosures per droplet (bottom) for $T = 2300$ K (initial conditions as in Figs. 5 and 6) and $T = 2600$ K (initial cond. as in Fig. 7).
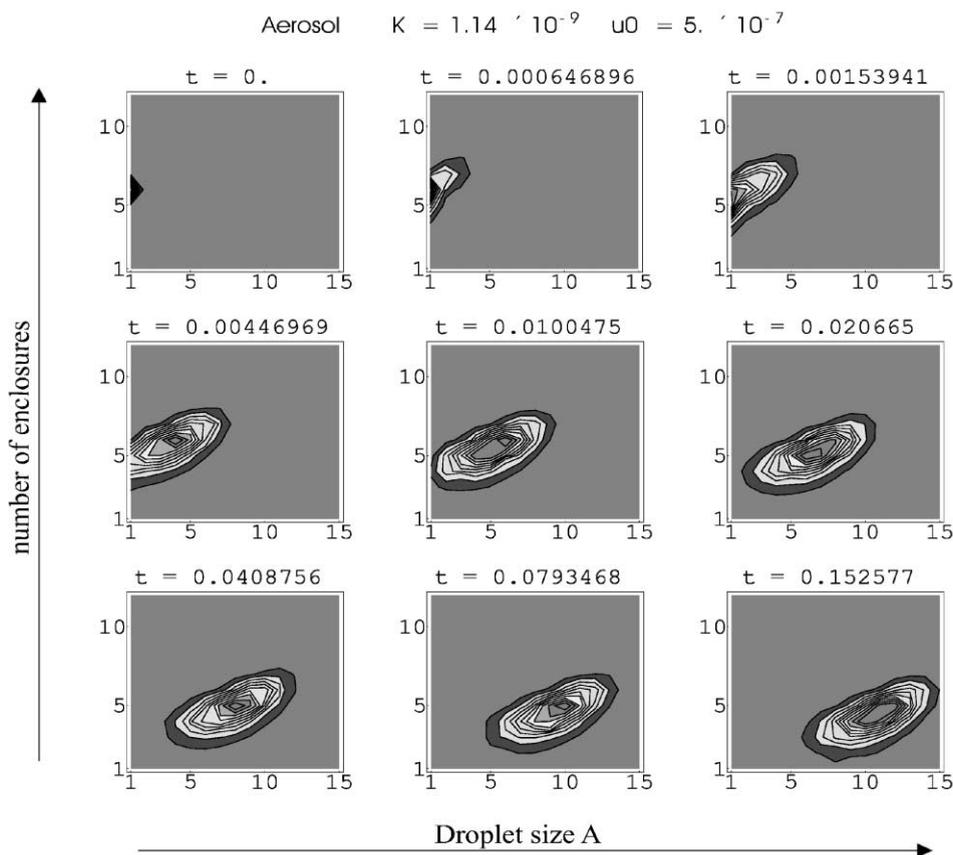
Fig. 9. Temporal evolution of v_α^A for $K = 1.14 \times 10^{-9}$, $u_0 = 5 \times 10^{-7}$ ($T = 2300$ K) for enclosure collision rate $\gamma_{m \to n}$ given by Eq. (28). Vertical axis: α, horizontal axis: A. The gray levels refer only to the relative values inside one plot. t is the actual time in seconds.

$\gamma_{m \to n}$ is too simple. Indeed, in the derivation of $\gamma_{m \to n}$, we have ignored the size distribution of the enclosures, as well as the finite size of the droplets, and in particular the tendency of the enclosures to stay at the edge of the droplets (see Fig. 1).

Clearly, we would like to see an increase in the enclosure collision rate, which could occur if the volume dependence in Eq. (6) was smaller. One justification would be that as we noted, experimental evidence suggests a migration of the enclosures to the surface, implying a surface diffusion of enclosures, or alternatively a decrease in the effective volume used in the denominator of Eq. (6). This argument would favor an exponent of 0.66 for V. We found that if we replace $\gamma_{m \to n}$ by

$$\tilde{\gamma}_{m \to n}(V) = \frac{K_0}{V^{1/3}} \frac{nm}{m - n} \tag{28}$$

we can find the desired behavior. The choice of the exponent $(1/3)$ is arbitrary and not justified by any physical considerations. Fig. 9 shows the result. Now, indeed, the number of enclosures decreases with increasing time.

The enhancement of the collision rate is not unjustified if we consider the surface effects discussed above as well as the fact that our present model assumes monodisperse enclosures. These results show that a better modeling of the inner droplet processes as well as the incorporation of a polydisperse enclosure model might allow for better agreement with the experiments.

Acknowledgements

Appendix A. Influence of concentration on collision frequency

Let us briefly reconsider our proceedings in Section 3.1, where we computed the collision probability for enclosures. The use of Eq. (5) is justified, if the enclosures can be considered as point particles, i.e. if their volume is very small compared to the droplet volume. This manifests itself in the definition of the number density of enclosures as $v = n/V$. If the enclosures assume a reasonable amount of the droplets volume, we have to consider the corrected number density

$$v_a = \frac{n}{V_a}$$

instead, where V_a is the volume that is indeed available for one enclosure. This idea comes from statistical thermodynamics, where one corrects the ideal gas law for the molecular volume, to arrive at the van-der-Waals-equation (Lee, Sears, & Turcotte, 1973). Following the arguments in Lee, Sears, and Turcotte (1973), we conclude that

$$V_a = V - 4cV,$$

where cV is the volume occupied by the enclosures. Replacing V by V_a, we arrive at the corrected collision frequency

$$\frac{1}{t_{m \to n}} = \gamma_{m \to n}(V) = \frac{K_0}{V(1 - 4c)} \frac{nm}{m - n}.$$

Thus, the probability of agglomeration increases with larger concentration c, i.e. for larger enclosures. Still, the equation is restricted to small concentrations—the available volume must be positive. It must be emphasized, though, that this correction does not change the dependence of $\gamma_{m \to n}$ on the volume.

Appendix B. The matrix $\mathscr{A}_{\alpha\beta}$

For the determination of the matrix $\mathscr{A}_{\alpha\beta}$, we consider

$$S_\alpha = \sum_{n=M_{\alpha-1}+1}^{M_\alpha} \left[\sum_{m=n+1}^{n_{\max}} \frac{nm}{m-n} N_m - \sum_{m=1}^{n-1} \frac{nm}{n-m} N_n \right].$$

With Eq. (13) and $n_{\max} = M_{\alpha_{\max}}$, we can write

$$
S_\alpha = \sum_{n=M_{\alpha-1}+1}^{M_\alpha} \left[\sum_{m=n+1}^{M_\alpha} \frac{nm}{m-n} N_m + \sum_{\beta=\alpha+1}^{\alpha_{\max}} \sum_{m=M_{\beta-1}+1}^{M_\beta} \frac{nm}{m-n} N_m - \sum_{m=1}^{n-1} \frac{nm}{n-m} N_n \right]
$$

$$
= \sum_{\beta=\alpha+1}^{\alpha_{\max}} \frac{1}{\mu_\beta} \sum_{n=M_{\alpha-1}+1}^{M_\alpha} \sum_{m=M_{\beta-1}+1}^{M_\beta} \frac{nm}{m-n} v_\beta - \frac{1}{\mu_\alpha} \sum_{n=M_{\alpha-1}+1}^{M_\alpha} \left[\sum_{m=n+1}^{M_\alpha} \frac{nm}{n-m} + \sum_{m=1}^{n-1} \frac{nm}{n-m} \right] v_\alpha.
$$

For the second expression, we have

$$
\sum_{n=M_{\alpha-1}+1}^{M_\alpha} \left[\sum_{m=n+1}^{M_\alpha} \frac{nm}{n-m} + \sum_{m=1}^{n-1} \frac{nm}{n-m} \right] = \sum_{n=M_{\alpha-1}+1}^{M_\alpha} \sum_{\substack{m=1 \\ m\neq n}}^{M_\alpha} \frac{nm}{n-m} = \sum_{n=M_{\alpha-1}+1}^{M_\alpha} \sum_{m=1}^{M_{\alpha-1}} \frac{nm}{n-m},
$$

where we have used that, due to symmetry

$$
\sum_{n=M_{\alpha-1}+1}^{M_\alpha} \sum_{\substack{m=M_{\alpha-1}+1 \\ m\neq n}}^{M_\alpha} \frac{nm}{n-m} = 0.
$$

We obtain finally that

$$
S_\alpha = \sum_{\beta=\alpha+1}^{\alpha_{\max}} \mathscr{A}_{\alpha\beta} v_\beta + \mathscr{A}_{\alpha\alpha} v_\alpha
$$

with the matrix elements given by Eq. (16).

Appendix C. The matrix $\mathscr{B}_{\alpha\beta}$

We write $N_m(U) = N_m$, $N_m(U - V) = \bar{N}_m$ and consider the quantity

$$
S_\alpha = \sum_{n=M_{\alpha-1}+1}^{M_\alpha} \sum_{m=1}^{n-1} N_m \bar{N}_{n-m}
$$

that appears in the summation of the first term on the right-hand side of Eq. (3) over the class α. This can be written as

$$
S_\alpha = s_\alpha - s_{\alpha-1},
$$

where

$$
s_\alpha = \sum_{n=2}^{M_\alpha} \sum_{m=1}^{n-1} N_m \bar{N}_{n-m} = \sum_{m=1}^{M_\alpha-1} \sum_{n=m+1}^{M_\alpha} N_m \bar{N}_{n-m} = \sum_{m=1}^{M_\alpha-1} \sum_{n=1}^{M_\alpha-m} N_m \bar{N}_n \quad \text{and} \quad s_0 = s_1 = 0.
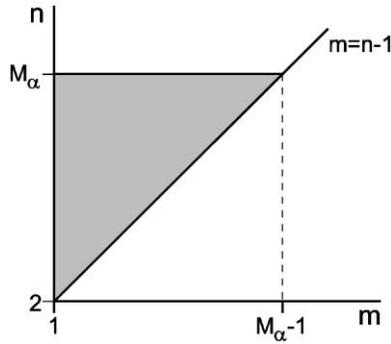$$

Fig. 10. Calculation of s_α: all points in the gray area appear in the summation.
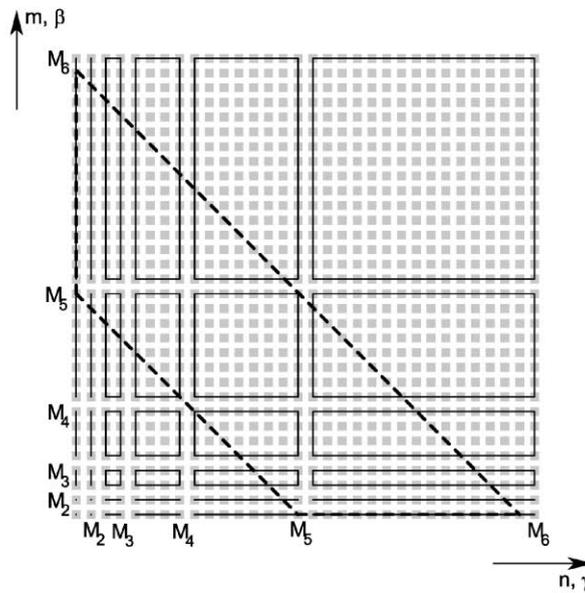

Fig. 11. Computation of S_6, see text for description.

The reversion of the order of summation is best understood by means of Fig. 10, that shows the area of summation for s_α. It also involves the substitution $(n-m) \to n$. The meaning of S_α is best read off from Fig. 11 which pictures the situation for the calculation of S_6:

s_6 is the sum over all points on and below the upper dashed diagonal, and s_5 is the sum over all points below (but not on) the lower dashed diagonal.

S_6 is the sum over all those points on and inside the dashed curve in the figure.

All points inside the rectangles $(1+M_{\beta-1}, M_\beta)(1+M_{\gamma-1}, M_\gamma)$ refer to values of $N_m \bar{N}_n = v_\beta \bar{v}_\gamma /(\mu_\beta \mu_\gamma)$, see Eq. (13). For the calculation of S_α we have to multiply $v_\beta \bar{v}_\gamma /(\mu_\beta \mu_\gamma)$ with the number of those points of the rectangles that lie inside the dashed region, and sum over all rectangles.

It is due to our peculiar choice (12) of the class width μ_α that S_α can be calculated easily as

$$S_\alpha = v_{\alpha-1}\bar{v}_{a-1} + \sum_{\beta=2}^{\alpha-2} \frac{3\mu_\beta^2}{2\mu_{\alpha-1}\mu_\beta}(v_{\alpha-1}\bar{v}_\beta + v_\beta\bar{v}_{\alpha-1}) + \frac{1}{\mu_{\alpha-1}}(v_{\alpha-1}\bar{v}_1 + v_1\bar{v}_{\alpha-1})$$

$$+ \sum_{\beta=2}^{\alpha-1} \frac{\mu_\alpha\mu_\beta - \frac{3}{2}\mu_\beta^2}{\mu_\alpha\mu_\beta}(v_\alpha\bar{v}_\beta + v_\beta\bar{v}_\alpha) + \frac{\mu_\alpha - 1}{\mu_\alpha}(v_\alpha\bar{v}_1 + v_1\bar{v}_\alpha).$$

Introducing the matrix $\mathscr{B}_{\alpha\beta}$ given by Eq. (8), we find finally

$$S_1 = 0,$$

$$S_\alpha = v_{\alpha-1}\bar{v}_{a-1} + \sum_{\beta=1}^{\alpha-1}(1 - \mathscr{B}_{\alpha\beta})(v_\alpha\bar{v}_\beta + v_\beta\bar{v}_\alpha) + \sum_{\beta=1}^{\alpha-2}\mathscr{B}_{\alpha-1,\beta}(v_{\alpha-1}\bar{v}_\beta + v_\beta\bar{v}_{\alpha-1}).$$

Note that $\mathscr{B}_{21} = 1/\mu_2 = 1$, so that $S_2 = v_1\bar{v}_1$.

Appendix D. The functions $I_{\alpha\beta}^A$

We compute

$$I_{\alpha\beta}^A = \int_{V_{A-1}}^{V_A} I_{\alpha\beta}(V)\,\mathrm{d}V = \frac{1}{2}\int_{V_{A-1}}^{V_A}\int_0^V \sigma(U, V-U)v_\alpha(U)v_\beta(V-U)\,\mathrm{d}U\,\mathrm{d}V$$

which after the substitution $V - U \to W$ can be written as

$$I_{\alpha\beta}^A = i_{\alpha\beta}^A - i_{\alpha\beta}^{A-1} \quad \text{with } i_{\alpha\beta}^A = \frac{1}{2}\int_0^{V_A}\int_0^{V_A-U}\sigma(U,W)v_\alpha(U)v_\beta(W)\,\mathrm{d}W\,\mathrm{d}U, \quad i_{\alpha\beta}^0 = 0.$$

The meaning of $I_{\alpha\beta}^A$ is best read off from Fig. 12 which shows the situation for the calculation of $I_{\alpha\beta}^6$: All points inside the rectangles $(V_{A-1}, V_A)(V_{B-1}, V_B)$ refer to values of $v_\alpha(U)v_\beta(W) = v_\alpha^A v_\beta^B/(\Delta_A\Delta_B)$, see Eq. (21). I_6 is the integral over the dashed curve in the figure. After replacing the number densities in the sections with the mean values (21) we find

$$I_{\alpha\beta}^1 = \frac{1}{2}\int_0^{V_1}\int_0^{V_1-U}\frac{\sigma(U,W)}{\Delta_1\Delta_1}\,\mathrm{d}W\,\mathrm{d}U\,v_\alpha^1 v_\beta^1,$$

$$I_{\alpha\beta}^2 = \frac{1}{2}\int_0^{V_1}\int_{V_1-U}^{V_1}\frac{\sigma(U,W)}{\Delta_1\Delta_1}\,\mathrm{d}W\,\mathrm{d}U\,v_\alpha^1 v_\beta^1 + \frac{1}{2}\int_0^{V_1}\int_{V_1}^{V_2-U}\frac{\sigma(U,W)}{\Delta_1\Delta_2}\,\mathrm{d}W\,\mathrm{d}U[v_\alpha^1 v_\beta^2 + v_\alpha^2 v_\beta^1],$$
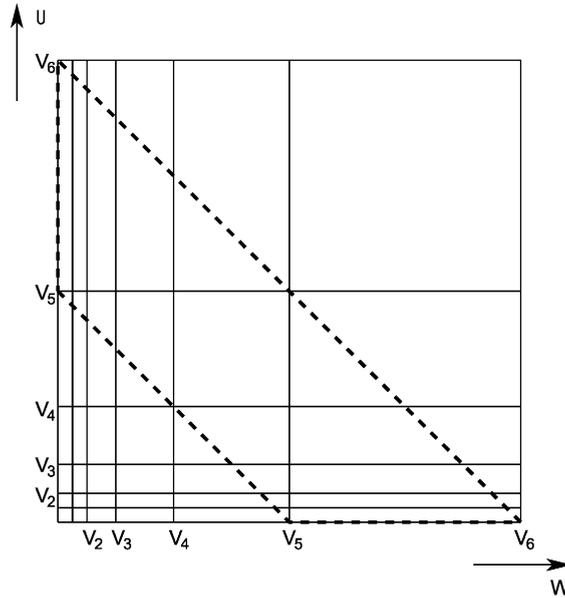
Fig. 12. Calculation of $I_{\alpha\beta}^A$, see text for details.

$$I_{\alpha\beta}^A = \frac{1}{2} \int_{V_{A-2}}^{V_{A-1}} \int_{V_{A-2}}^{V_{A-1}} \frac{\sigma(U,W)}{\Delta_{A-1}\Delta_{A-1}} \, \mathrm{d}W \mathrm{d}U v_\alpha^{A-1} v_\beta^{A-1}$$

$$+ \frac{1}{2} \sum_{B=1}^{A-2} \int_{V_{B-1}}^{V_B} \int_{V_{A-1}-U}^{V_{A-1}} \frac{\sigma(U,W)}{\Delta_{A-1}\Delta_B} \, \mathrm{d}W \, \mathrm{d}U [v_\alpha^{A-1} v_\beta^B + v_\alpha^B v_\beta^{A-1}]$$

$$+ \frac{1}{2} \sum_{B=1}^{A-1} \int_{V_{B-1}}^{V_B} \int_{V_{A-1}}^{V_A-U} \frac{\sigma(U,W)}{\Delta_A \Delta_B} \, \mathrm{d}W \, \mathrm{d}U [v_\alpha^A v_\beta^B + v_\alpha^B v_\beta^A] \quad (A \geqslant 3).$$

Introduction of the mean collision frequencies (24) yields $I_{\alpha\beta}^A$ in the form of Eq. (23).

References

Biswas, P., Wu, C. Y., Zachariah, M. R., & McMillen, B. K. (1997). In situ characterization of vapor phase growth of iron oxide-silica nanocomposite—Part II. Comparison of a discrete-sectional model predictions to experimental data. *Journal of Materials Research*, *12*, 714.

Biswas, P., & Zachariah, M. R. (1997). In situ immobilization of lead species in combustion environments by injection of gas phase silica sorbent precursors. *Environmental Science and Technology*, *31*, 2455.

Biswas, P., Yang, G., & Zachariah, M. R. (1998). In-situ processing of ferroelectric materials from lead streams by injection of gas-phase titanium precursors. *Combustion Science and Technology*, *134*, 183.

Ehrman, S. H., Friedlander, S. K., & Zachariah, M. R. (1998). Characterization of SiO_2/TiO_2 nanocomposite aerosol in a premixed flame. *Journal of Aerosol Science*, *29*, 687.

Ehrman, S. H., Aquino-Class, M. I., & Zachariah, M. R. (1999). Effect of temperature and vapor-phase encapsulation on particle growth and morphology. *Journal of Materials Research*, *14* (4), 1664–1671.

Ehrman, S. H., Friedlander, S. K., & Zachariah, M. R. (1999). Phase segregation in binary SiO_2/TiO_2, SiO_2/Fe_2O_3 aerosols formed in a premixed flame. *Journal of Materials Research*, *14*, 4551.

Friedlander, S. K. (2000). *Smoke, dust and haze*. Oxford: Oxford University Press.

Fuchs, N. A. (1989). *The mechanics of aerosols*. New York: Dover.

Hunslow, M. J., Ryall, R. L., & Marshall, V. R. (1988). A discretized population balance for nucleation, growth and aggregation. *AIChE Journal*, *34*, 1821.

Kingery, W. D., Bowen, H. K., & Uhlmann, D. R. (1976). *Introduction to ceramics*. New York: Wiley.

Koch, W., & Friedlander, S. K. (1990). The effect of particle coalescence on the surface area of a coagulating aerosol. *Journal of Colloid and Interface Science*, *140*, 419–427.

Landgrebe, J. D., & Pratsinis, S. E. (1990). A discrete-sectional model for particulate production by gas-phase chemical reaction and aerosol coagulation in the free-molecular regime. *Journal of Colloid and Interface Science*, *139*, 63–86.

Lee, J. F., Sears, F. W., & Turcotte, D. L. (1973). *Statistical thermodynamics*. Reading, MA: Addison-Wesley.

McMillin, B. K., Biswas, P., & Zachariah, M. R. (1996). In situ characterization of vapor phase growth of iron oxide-silica nanocomposite; Part I: 2-D planar laser-induced fluorescence and Mie imaging. *Journal of Materials Research*, *11*, 1552–1561.

Park, S. H., Lee, K. W., Otto, E., & Fissan, H. (1999). The log-normal size distribution theory of Brownian aerosol coagulation for the entire particle range: Part I: Analytical solution using the harmonic mean coagulation kernel. *Journal of Aerosol Science*, *30*, 3–16.

Xiong, Y., & Pratsinis, S. E. (1993). Formation of agglomerate particles by coagulation and sintering—Part I. A two-dimensional solution of the population balance equation. *Journal of Aerosol Science*, *24*, 283.

Zachariah, M. R., Aquino-Class, M., Shull, R. D., & Steel, E. (1995). Formation of superparamagnetic nanocomposites from vapor phase condensation in a flame. *Nanostructured Materials*, *5*, 383.

Zachariah, M. R., Shull, R. D., McMillin, B. K., & Biswas, P. (1996). *In situ characterization and modeling of the vapor phase growth of a superparamagnetic nanocomposite*. Nanotechnology, *622*, 42–63 (Chapter 3).